Effect of Multifrequency Forcing on the Near-Field Development of a Jet

T. T. Ng* and T. A. Bradley†
University of Notre Dame, Notre Dame, Indiana

Flow visualization and hot-wire measurements are used to study the effect of acoustically forcing a jet with low-level disturbances containing more than one frequency component. Specifically for this study, forcings with combined frequencies at a ratio of 1 to 2 (1-2) and a ratio of 1 to 3 (1-3) are examined. For the 1-2 forcing, if the initial growth of the longer wave is sufficiently strong compared with that of the shorter wave, three manners of vortex merging can be observed: 1) pairing between two vortices of similar size, 2) pairing between two vortices of different size, and 3) vortex "tearing." Both the initial phase angle and the Strouhal number play a key role in determining the manner of vortex merging. When forced at the condition where the first mode is close to the initially most amplified frequency, no vortex tearing can be observed, and vortex pairing occurs mostly between vortices of similar size. The phase angle affects mainly the pairing location under this situation. For the 1-3 forcing, three merging modes are identified. The initial phase angle has a major effect in determining the merging mode. Regardless of the mode of forcing, the specific total energy tends toward the same asymptotic value.

Introduction

THE effect of flow disturbances on shear flow development is a phenomenon of major practical importance because of the potential applications for problems such as combustion and jet noise control. Free shear flows, which include jets, plane shear layers, and wakes, are especially sensitive to low-level disturbances that affect the vortex evolution process. Initially, periodic forcing was used primarily as a means of providing phase references in many shear flow experiments; however, it was soon realized that low-level forcing could also be used as a relatively easy means of controlling a flow.

Roshko[1] demonstrated the existence of large-scale, organized structures, even in highly turbulent shear flows. While the exact nature of these large structures is still not known, it is generally believed that they play a major role in fluid entrainment and mixing in a shear layer. Winant and Browand[2] showed that the vortex coalescence process, referred to later as pairing, is mostly responsible for the growth of a shear layer, although later Hernan and Jimenez,[3] through digital image analysis, indicated that entrainment by the large vortices rather than pairing is the main mechanism for shear-layer growth. Miksad[4,5] studied the nonlinear interactions in the transition region of a free shear layer by acoustically forcing the flow at two frequencies of comparable growth rates. In addition to the forcing frequencies and their sum and difference modes, harmonics and subharmonics of the forcing frequencies were observed to grow and interact with others to generate additional components. Most of the later studies, such as Zaman and Hussain,[6,7] Ho and Huang,[8] and Oster and Wygnanski,[9] concentrate mainly on monotone forcing. In general, the results indicated that the shear-layer spreading rate could be manipulated effectively by subharmonic forcing. Enhancement or suppression of layer growth is possible by forcing at appropriate amplitudes and wavelengths. Much of the work up to 1984 on forced shear layer was summarized by Ho and Huerre.[10] More recently, Wygnanski and Petersen[11] discussed several aspects of shear layers and explored the possibility of combined mode forcing to extend the range over which the flow could be controlled.

The initial development of a jet is similar to that of a plane shear layer. The most significant difference is that while the initial layer thickness forms a length scale for both flows, the diameter of the jet represents a second length scale that does not exist in a plane shear layer. The presence of the diameter leads to the possibility of a large number of azimuthal instability modes. The vortex rollup can also induce perturbations across the potential core of a jet. In a typical plane shear-layer experiment, however, the test section will have a finite cross section and thus may introduce some of the effects not present in a truly two-dimensional plane shear layer.

In a typical jet flow, a potential core will exist for several diameters downstream from the exit. Near the exit, the jet will respond to flow disturbances as dictated by the initial velocity profile in the shear layer. At this stage, the axisymmetric waves tend to have a higher growth rate, and the flow is usually dominated by axisymmetric vortex rings. For a specific local condition, the energy growth rate will peak at a certain frequency and diminish continuously away from that frequency. While forcing near the peak frequency will be the most efficient way to enhance the initial layer growth, forcing at another frequency at sufficiently high initial amplitude can result in a direct response of the layer to that particular forcing frequency.

Furthermore, alignment of the vorticity fields of a response frequency and its subharmonics will dictate the manner in which further growth of the layer will take place. This has been demonstrated by several analytical and numerical studies (e.g., Refs. 13-16), though few experimental results (e.g., Ref. 12) are presently available. In an "unforced" or naturally forced flow, the wave with the proper amplitude and phase alignment will be amplified the most. In a flow with forcing at more than one frequency, with controls over the characteristics of each frequency component, the flow can be induced to respond in a large variety of ways. Near the end of the potential core, the centerline velocity fluctuation reaches a maximum, with a reported Strouhal number $f_p D/U_j$ ranging from 0.25 to 0.85. This is commonly referred to as the preferred mode or jet-column mode, although it is not clear that the basic instability associated with the preferred mode is different from that of the shear-layer mode. After the potential core diminishes, the axisymmetric waves are suppressed, and the helical modes become the dominant instability modes.

Received July 14, 1986; revision received July 1, 1987.

*Assistant Professor.
†Graduate Student.

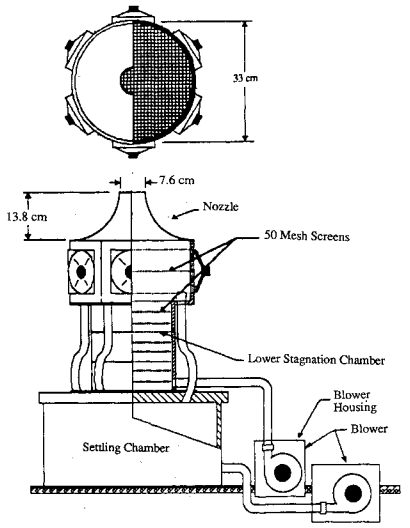

Fig. 1 Schematic of the jet flow apparatus. For the present study, only the blower supplying the lower stagnation chamber was used.

Under proper forcing conditions, different instability modes can also be induced to interact, as demonstrated by Wygnanski and Petersen.[11]

The objective of this study is to examine the effect of forcing a jet with more than one spectral component. The present report will focus on the development of the jet before the disappearance of the potential core. Forcing is produced acoustically with controls on phase relations and frequencies. Results from flow visualization and hot-wire measurements will be presented.

Apparatus

Jet Flow Apparatus

The experiment was carried out in the jet flow apparatus shown in Fig. 1. The apparatus can be configured to operate in either the coaxial or the single-jet mode. The present experiment was performed in the single-jet mode, with a nozzle having a 7.6-cm-diam outlet and a 33-cm-diam base connected to a 51-cm high stagnation chamber. The nozzle wall thickness was about 1/4 mm. The nozzle contraction occurred over a relatively short distance. This allowed a low initial shear-layer thickness to diameter ratio; however, the quick contraction and the nozzle shape resulted in a slightly U-shaped velocity profile at the potential core of the flow at the nozzle exit. In general, the centerline velocity U_j was about 5–10% lower than the maximum mean velocity around the edge at the exit. This, however, was not expected to have a significant effect on the shear-layer development, since most of the vorticity was still contained within the shear layer. Several layers of 50-mesh screens were placed inside the stagnation chamber to damp out larger flow structures. Air flow was supplied by a variable-speed axial blower. The nozzle assembly was placed inside a large rectangular enclosure made of plastic sheet on a wooden frame to minimize disturbances from random ambient air movement.

Controlled velocity perturbation was facilitated by a 4 in. speaker mounted on the side wall of the settling chamber. The outlet of the speaker opening was lined with a screen to break up large-scale waves. The finite volume of the chamber and the reflection of the acoustic wave from the side walls were two of the concerns that could affect the tone quality of the perturbation. To minimize these problems, five additional speakers (nonactive) were mounted on the stagnation chamber to create, in effect, a semiflexible sidewall.

At the testing flow (4 m/s at exit centerline), the centerline disturbance level was 0.4% without forcing. The flow chamber acoustical response was measured by using a B&K Type 4135 condenser microphone (frequency response flat from 20 Hz to 2 kHz) and forcing the speaker over a range of frequencies. During the test, placement of the microphone was varied from inside the chamber to near the exit, and the flow speed was varied over a range to check possible input from the fan. In all cases, the chamber showed a similar frequency response. The response rose steadily from 20 Hz to a gentle peak at about 66 Hz and gradually leveled off at higher frequencies. This response characteristic was used later on to help quantify the initial forcing amplitudes for the different cases being studied.

Generation of Forcing

It would be difficult to maintain definite phase and amplitude relaxations among spectral components of the forcing signal if more than one signal generator were used to generate the signal. Thus, the input signal was initially created by combining linearly spectral components (or sine functions) of desired phases and amplitudes in a Macintosh computer. The signal was then output through a D/A converter, filtered by a DISA 55D25 filter to remove undesired high-frequency components, and fed into a 100-W ac amplifier that drove the speaker. The various devices along the signal path caused phase shifting of each of the spectral components of the forcing signal, with the amount of shifting being dependent on component frequency. This resulted in velocity perturbation having different spectral phase relations from the signal created originally in the computer. The decreased response of the speaker at low frequency and the acoustical characteristics of the flow chamber also resulted in modification of the initial forcing amplitudes of the frequency components. These, however, could be compensated for during formulation of the signal in the Macintosh computer if desired, although no such attempt was made during the course of the present experiment, and the phase relations referred to later on in the report were the original phase relations as input at the computer.

Equipment

Flow visualization studies were carried out using two different light illumination techniques. The flow was seeded with kerosene vapor created by an evaporation-condensation process for light scattering. One visualization study was performed by illuminating the flow with a sheet of laser light produced by passing the light beam from a 4-W argon ion laser through a cylindrical lens. This method allowed a clear view of the flow cross section. Another visualization study was performed by illuminating the flow with a strobe light at the forcing frequency or its subharmonics. The strobe light illumination method has the advantage of being able to "freeze" the flow at various stages of development by adjusting the relative phase between the stroboscope and the forcing signal. By synchronizing the strobe with the still camera, a photographic record could then be obtained. This method allowed the flow to be studied more economically and conveniently over a wide range of conditions. Both methods were used in the course of this study, although only the pictures from the strobe light technique will be shown.

Velocity measurement was performed using a DISA 55P01 hot wire in conjunction with a DISA 55M01 anemometer and a DISA 55D25 signal conditioner. The hot wire was calibrated against a pitot-static tube connected to a Setra 339B electronic manometer with a four-digit readout and a range of 0–0.55 in. of water. The calibration data were eventually curve-fitted to a polynomial to a correlation coefficient of better than 99.5%. The data were then extrapolated to give calibration at the lower velocity range. Later on in the experiment, a DISA x-wire was used.

The hot wire was mounted on a two-dimensional traverse with stepping motor control on the horizontal motion. Data were recorded by a PDP 11/23 based data acquisition system with a 12-bit A/D converter. At each location 4000 samples were taken at the rate of 500 samples/s with the low-pass filter on the DISA 55D25 set at 200 Hz. Data processing was carried out using a PDP 11/34 computer. Cross-wire data were taken

in a similar fashion, except that the forcing signal was also recorded to provide phase reference for phase-locked data reduction.[17]

Results

Initial Conditions

As mentioned before, the response of a shear layer to an artificial forcing depends on several parameters of the forcing: the frequency content, the amplitude of forcing, and the relative phase angles among the frequency components and their relative amplitudes. While it is often inappropriate or impossible to isolate the effect of each of these parameters for a given flow situation, due to the inevitable time and resource limitations, the present study concentrates mainly on effects of the frequency content and relative phase angles. The experiment was conducted at a centerline exit velocity of 4 m/s. The overall forcing level u_0' was kept constant at 1.4% of the centerline velocity, and the initial amplitude of each of the frequency components was the same order. For a pure tone forcing, the harmonic distortion of the forced disturbance at the nozzle exit as measured by the amplitudes of the higher harmonics was in general on the order of 1% for the frequencies investigated. The initial condition for each case being studied is indicated on the figures and in the corresponding discussion.

Data Reduction

Mean and rms velocities U and u, respectively, were obtained directly from time-averaging the hot-wire measurements. The initial momentum thickness θ_0 was obtained by extrapolation to the origin at the nozzle outlet. Due to the slightly U-shaped core profile, the momentum thickness was evaluated by integrating the mean velocity from the point r_0 of maximum velocity $U_{\max}$ to the radial position r_1, where the velocity leveled off to approximately zero:

$$\theta = \int_{r_0}^{r_1} U/U_{\max}(1 - U/U_{\max})\, dr$$

The initial momentum thickness θ_0 was estimated to be 1 mm without forcing. The initial most amplified frequency f_n was determined by observing the initial layer growth under monofrequency forcing and was about 60 Hz, corresponding to an initial Strouhal number ($St_\theta = 2f\theta/U_j$) of 0.03.

The spectral energy distribution at each spatial position was obtained using the fast Fourier transform (FFT). To avoid the ambiguity in determining the radial poisition for terminating the integration (so as to prevent the disturbances in the ambient air from distorting the actual energy distribution in the jet), total "energy" integral E_t at a given streamwise location was evaluated by integrating the energy over the area from the center to the radial position $r_{0.05}$ (defined as where the mean velocity is 5% of the jet centerline velocity):

$$E_t = \int_{r_0}^{r_{0.05}} (u^2) 2\pi r\, dr$$

The 5% limit was chosen so that a definite local limit could be used for all streamwise locations. The disturbance level in the ambient air in general was very low. However, if an integration was performed over a very large radius, the contribution from the ambient disturbances could become significant.

The energy integral was scaled by A_θ:

$$A_\theta = \int_{r_0}^{r_{0.05}} U/U_{\max}(1 - U/U_{\max}) 2\pi r\, dr$$

This quantity could be interpreted as an area scale for the shear layer.

Discussion

Single-Mode Forcing

Pure tone forcing has been studied rather extensively by various researchers. As indicated by Ho and Huang,[8] forcing at appropriate Strouhal numbers can lead to different modes of "pairing" of the vortices in a shear layer. The single-frequency forcing results obtained during this study in general agree with those of Ho and Huang and thus will not be discussed in detail. The discussion will be concentrated on the cases of forcing with combined frequencies at a ratio of 1 to 2 (1–2 forcing) and a ratio of 1 to 3 (1–3 forcing). One observation during flow visualization study is that when forced at more than one frequency, the vortex merging process is highly localized and can be "frozen" visually in space by adjusting the phase and the frequency of the strobe light. In a monofrequency forced layer, the lack of control on the phase relation leads to a somewhat less (though still highly) localized vortex merging process that cannot be frozen as readily by the strobe light.

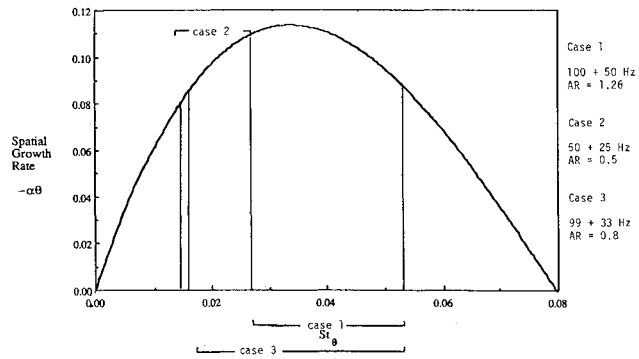

Fig. 2 Forcing conditions for the three cases studied. Spatial growth rate from a linear theory (Monkewitz and Huerre[18]) was used as a qualitative model.

1-2 Forcing

While the process being studied is nonlinear in nature, the growth curve from a linear stability theory is used in Fig. 2 as a model to indicate qualitatively the relative positions of the forcing frequencies in the cases studied. In a shear layer, a growth mode at higher frequency will saturate earlier than the lower one. For convenience of discussion, the former will be referred to as f (first wave), and the latter as s (second wave).

The growth rate and saturation point of any spectral component in a shear layer depend on its Strouhal number and initial amplitude and also in the way in which energy is exchanged among components. For instance, the fundamental subharmonic energy exchange is dependent on the effective phase difference, $2\phi_s - \phi_f - \phi_0$,[15] where ϕ_s and ϕ_f are the phase angles of the subharmonic and the fundamental and ϕ_0 is the initial phase difference. The development of the layer is therefore dependent on the initial forcing signal phase difference ϕ_i that determines ϕ_0.

Figures 3a–3c show the flow visualization results of simultaneously forcing at f of 100 Hz and s of 50 Hz at different ϕ_i. The forcing amplitude ratio (AR) between s and f was equal to 1.26, and u_0' was 1.4%. The pictures were obtained by varying the frequency and phase of the strobe light relative to the forcing and thus visually freezing the spatial development of the flow. For 1-2 forcing, depending on the initial Strouhal numbers (hence the growth rates) of the components and their relative phase angles, three merging modes were observed. In the first mode, demonstrated by Fig. 3a where $\phi_i = 0$, small vortices roll up at the f frequency and growth to nearly equal size before they pair. As ϕ_i increases, such as in the case of $\phi_i = 62$ deg shown in Fig. 3b, the vortices will initially roll up at two distinctly different scales. In the second merging mode, the small vortex will either pair with the leading or the trailing larger vortex. Figure 3c shows the extreme case (with $\phi_i = 152$ deg) at which the f wave has little time to grow and only a small "ripple" forms in the region between the two larger vortices before it is entrained by the leading vortex. Vortex rollup occurs essentially directly at the s

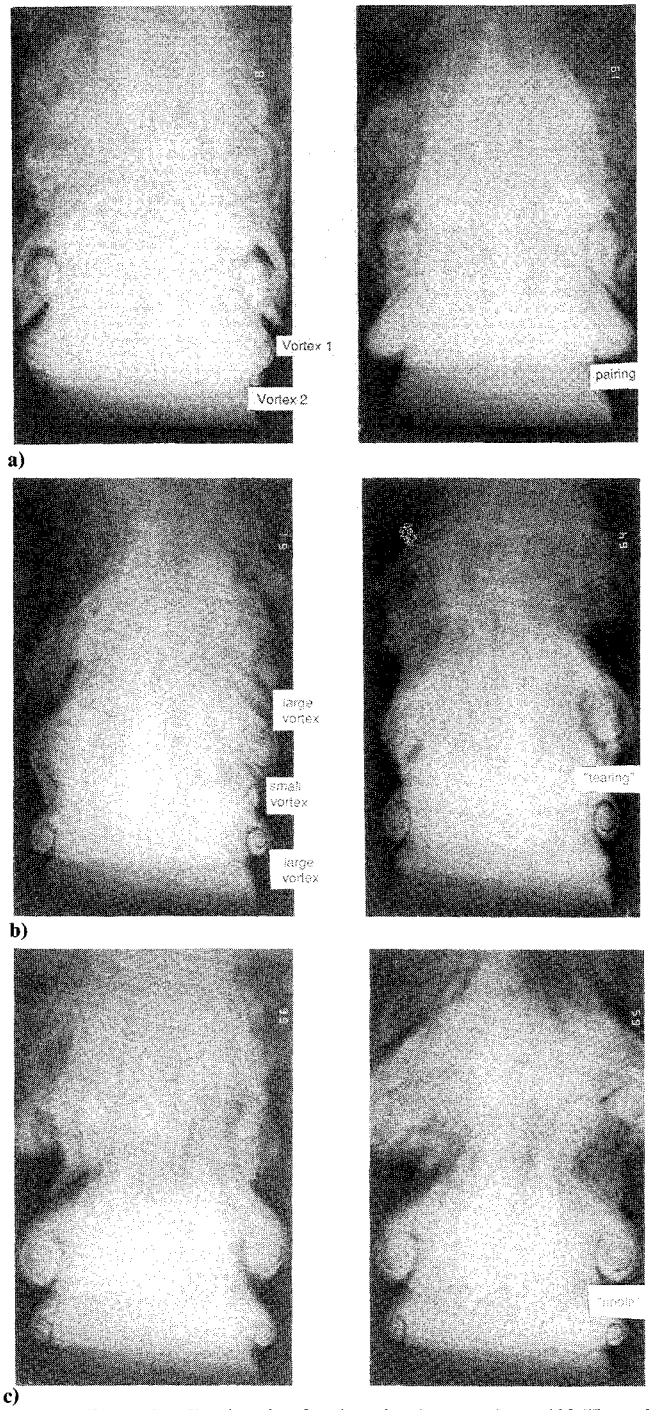

Fig. 3 Flow visualization for forcing simultaneously at 100 Hz and 50 Hz with an amplitude ratio of 1.26. Overall forcing level was 1.4%. Phase angles are a) $\phi_i = 0$ deg, b) $\phi_i = 62$ deg, c) $\phi_i = 152$ deg.

frequency. In the third merging mode at a ϕ_i near 62 deg, the small vortex will be "torn" up by the two adjacent larger vortices. However, this event is relatively unstable, and even a few degrees of deviation from this ϕ_i or any small disturbances will result in a switch to the second merging mode.

As will be explained, these three different merging modes are direct results of the different growth rates of the forcing frequency components and their evolutions and mutual interaction downstream. Referring to Fig. 2, when forcing at 100 and 50 Hz, the s mode is initially left of and close to the f_n and at a higher growth rate than the f mode, which is to the right of f_n and closer to the neutral point. As the layer thickens, the s growth rate increases to a peak value and then decreases. The f mode, on the other hand, decreases continuously until it reaches the saturation point. At the same

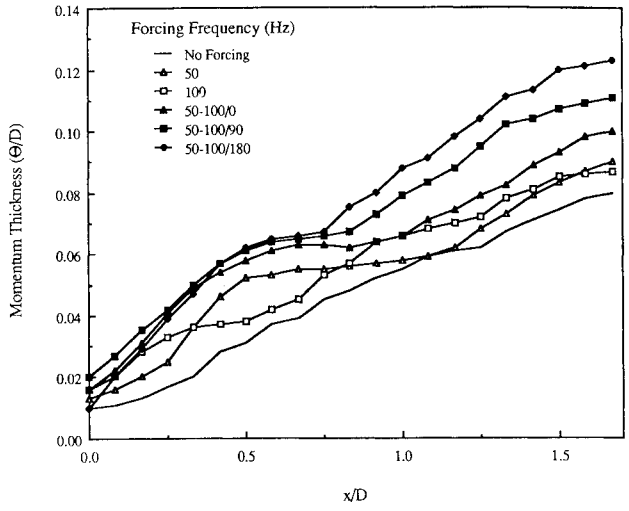

Fig. 4 Momentum thickness development for forcings at a) 50 Hz; b) 100 Hz; c) 100 + 50 Hz/0 deg phase angle; d) 100 + 50 Hz/90 deg; e) 100 + 50 Hz/180 deg; overall forcing level = 1.4%, AR = 1.26.

time, the s wave interacts with the f wave by exchanging energy, with the efficiency of exchange being dependent on the phase alignment of the two frequency waves. When the two waves are in phase, as in mode 1, the s wave reinforces the f wave evenly, and the pairing process involves two f vortices of equal size. As the phase difference increases, the s wave becomes more efficient in reinforcing one f vortex than the other. Coupling with the decreasing f growth rate due to layer thickening, the straining field of the larger vortex causes pairing to occur between two vortices of different size (mode 2). In the extreme case, as in Fig. 3c, the f mode has little opportunity to grow before saturation and vortex rollup occurs essentially at s. Mode 3 represents the situation at which f and s are in exact antiphase. The s wave reinforces every other f vortex, resulting in a small f vortex formed between two larger vortices of equal strength. The straining field associated with the two larger vortices acts evenly on the f vortex, and eventually it is torn instead of pairing with either one. In general, mode 2 will be the most probable pairing mode, since it occurs over a wide range of phase angle, while modes 1 and 3 will be relatively rare due to the specific phase requirements. The numerical simulations by Patnaik et al.[13] and Riley and Metcalfe[14] show similar relations between pair modes and phase alignment.

Another interesting observation from flow visualization (by noting the position where two vortices are aligned side by side) is that as ϕ_i increases, pairing between the s vortices farther downstream occurs sooner. This was confirmed by the momentum thickness shown in Fig. 4. Several conclusions can be drawn from the figure. Forcing at the two frequencies results in a faster growth of the layer than forcing by either frequency alone at the same initial overall forcing level. In contrast to several experiments at very low forcing levels, the initial layer thickness is altered by forcing. This alteration also shows up in most of the other cases that have been studied, with the degree of alternation depending strongly on the forcing conditions. Nevertheless, this suggests that local separation of the flow may have occurred slightly upstream of the exit, causing the layer to oscillate. Saturation of the f mode is difficult to identify in the momentum thickness due to the rapid growth of the s mode, and the growth to s saturation is more or less continuous. The saturation level is affected by ϕ_i, which also affects, to a lesser extent, the saturation location of the s mode due to the different ways of interaction between the f and the s waves. More interestingly, the different vortex merging conditions also cause sufficient modification of the shear flow to affect the growth rate of the subharmonic of the second mode ($s/2 = 25$ Hz), perhaps through thickening of the layer or modification of the local velocity profile, or both. The

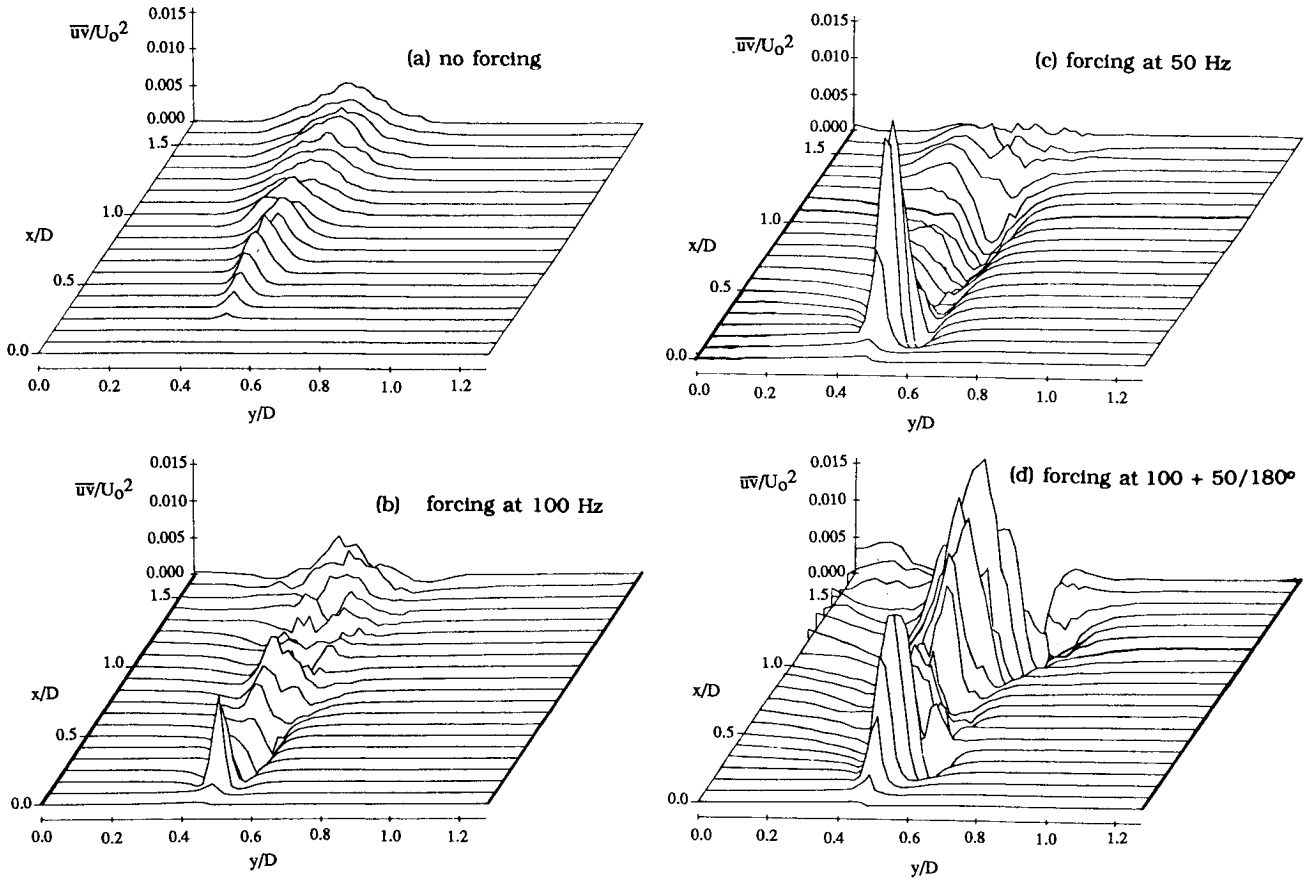

Fig. 5 Reynolds stress comparison among a) no forcing; b) forcing at 100 Hz; c) forcing at 50 Hz; and d) forcing at 100 + 50 Hz 180 deg.

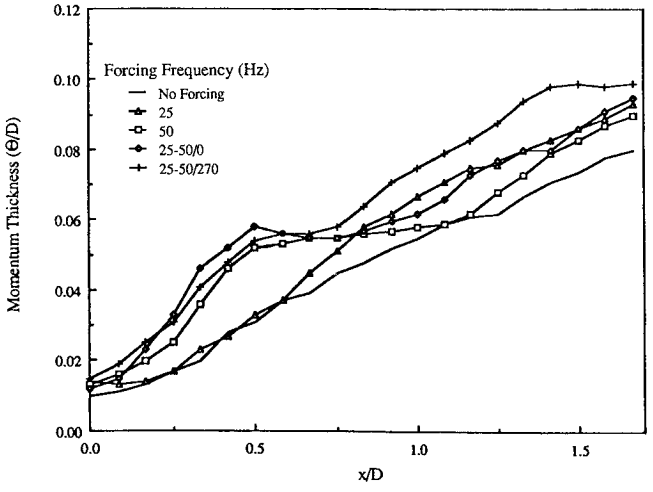

Fig. 6 Momentum thickness development for forcings at: a) 25 Hz; b) 50 Hz; c) 50 + 25 Hz/0 deg; d) 50 + 25 Hz/257 deg; overall forcing level = 1.4%; AR = 0.5.

$s/2$ energy growth rate increases when ϕ_i is varied from 0 to 180 deg as revealed by the spectral data,[17] with the corresponding increase in the layer thickness as shown in Fig. 4. In comparison with forcing at s alone, the addition of the f component causes both an increase in f saturation-layer thickness and a more rapid growth of the $s/2$ mode. The Reynolds stress plotted in Fig. 5 further confirms the observation. Forcing at f and s results in an initial peak corresponding to the growth of both the f and the s modes. This peak is similar to the peak for s growth when forced at s alone. Forcing at f and s, however, causes a large second rise starting at $x/d = 1$, whereas forcing at s alone show no second rise. The second rise is associated with the development of the $s/2$ mode, making the layer more effective in extracting energy from the mean flow.

Forcing at 50 Hz (f) and 25 Hz (s) with an AR of 0.5 was also investigated. As shown in Fig. 2, in this forcing case, the f frequency is close to f_n, and its initial growth rate is higher than that of the s mode. Coupled with the difference in initial forcing level, the f mode will therefore grow at a more rapid rate than the s mode. Flow visualization showed that pairing occurred between f vortices of either similar size or with a small difference in size, depending on ϕ_i, while the vortex tearing mode was never observed. Furthermore, the relative difference in vortex sizes at a given ϕ_i is smaller than in the previous case. This is because the more energetic initial growth of the f vortex in comparison with the s wave results in the influence of the s wave being reduced accordingly. The reinforcement from the s wave cannot strengthen every other f vortex in the vortex train to the extent that vortex tearing can occur before the necessary antiphase relation is dispersed. Zhang et al.[12] also observed that for a mixing layer excited at f_n and $f_n/2$ at antiphase, the tearing process seldom occurs; rather, the merging location becomes randomly distributed, as opposed to forcing at other phase angles. This observation agrees with the present results.

However, ϕ_i does have an effect on the eventual vortex merging location. Figure 6 shows the momentum thickness development of forcings at 50 and 25 Hz simultaneously, with ϕ_i of 0 and 270 deg. Single-mode forcing and the unforced flows are included for comparison. The figure shows that the first mode saturates at a similar location and thickness whether the layer is forced at f alone or a combined forcing of f and s. The growth of the s mode, on the other hand, is affected by ϕ_i. For $x/d < 0.6$, the s layer alone grows much like the unforced layer, while the f-s layer initially grows rapidly due to the f component. After f-mode saturation, the layer grows at different rates, depending on ϕ_i. The spreading of the layer is the slowest when there is no initial s forcing. Forcing at the f-s/0 phase shows a growth rate similar to forcing at s alone. With a ϕ_i of 270 deg, the s wave has a more favorable

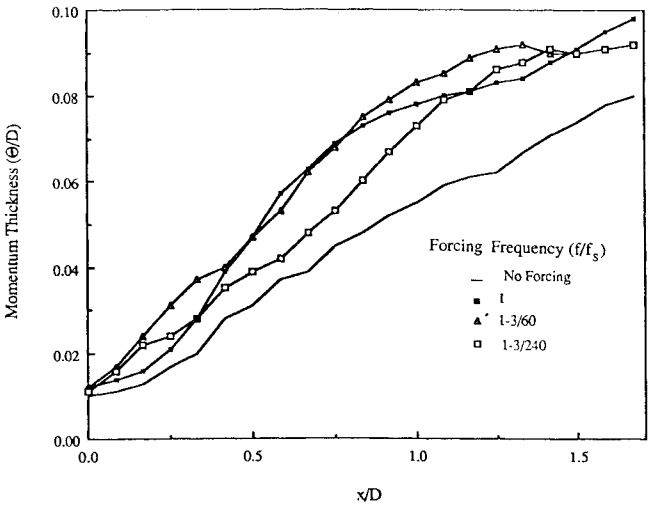

Fig. 7 Momentum thickness development for forcing at a) 33 Hz; b) 99 + 33 Hz/60 deg; and c) 99 + 33 Hz/240 deg.

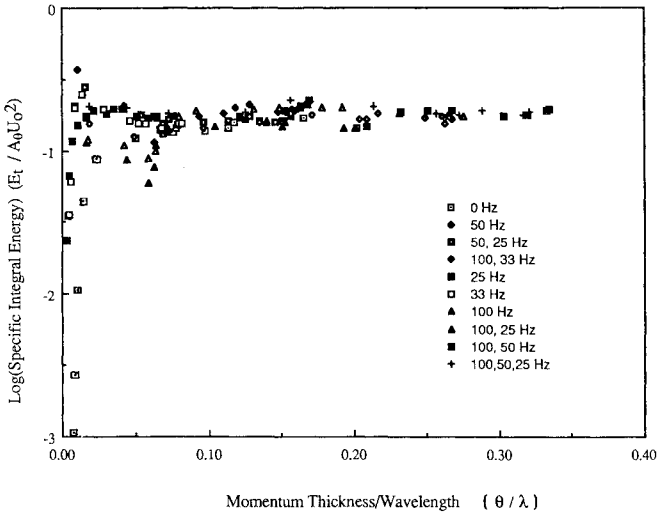

Fig. 8 Specific energy ($E_t/A_\theta U_0^2$) as a function of local momentum thickness (θ/λ); overall forcing level = 1.4%; $\phi_i = 0$ for all multifrequency cases.

alignment relative to the *f* wave, and the layer grows more rapidly due to the growth of the *s* wave. The same trends in the growth of momentum thickness of a circular jet under bimodal excitation was also shown numerically by Mankbadi.[15]

Forcing at 1-3

Forcings at 99 Hz (*f* mode) and 33 Hz (*s* mode) at an amplitude ratio of 0.8 and at various ϕ_i were examined. As shown in Fig. 2, the initial growth rates of the two forcing components are comparable. Due to the shorter wavelength of the *f* mode, saturation vortices (*f* vortices) will form initially at the higher frequency. Subsequently, three modes of merging can be identified from flow visualization. In the first mode, for three initial vortices that will eventually merge, the two leading vortices (1 and 2) will pair first and then merge with the trailing vortex (3). In the second mode, vortices 2 and 3 will pair first and then merge with the leading one. In the third mode, all three vortices will merge simultaneously. For most of the phase angles, two vortices merge first, and the resulting vortex merges with the third one. Only for a small range of phase angles (235-250 deg) do the three vortices merge at the same time. Flow visualization shows that for forcing phase angles between 250 deg and 0 deg, the bottom two vortices pair first and then merge with the top vortex. For the cases studied, the *f* vortices are all of similar scale, regardless of the ϕ_i. This indicates that the growth and saturation of the *f* wave are insensitive to the phase alignment of the *s* wave under this forcing condition. The main role of ϕ_i is to influence the eventual merging mode and location of the *f* vortices. Merging of modes 1 and 2 is caused by alignment of the *s* wave between two *f* vortices that induces them to pair. In mode 3, the *s* wave aligns on top of the middle vortex, thus causing the other two vortices to roll around and merge with the middle one simultaneously.

The momentum thickness development is shown in Fig. 7 for two different ϕ_i. The cases of no forcing and forcing at *s* alone are included for comparison. As indicated in the figure, the initial development of the layer due to the *f* mode is essentially indepenent of the phase angle. After saturation of the *f* mode, merging of two *f* vortices for $\phi_i = 60$ deg causes the layer to continue to thicken. For the cases of $\phi_i = 240$ deg, where three *f* vortices will eventually merge simultaneously, the development in layer thickness is slower by comparison due to the lack of vortex merging. Eventually, when three vortices merge at $x/d = 1.4$, the layer attains the same thickness as in the case of $\phi_i = 60$ deg.

Energy Integral

The total energy integrals for different modes of forcing are plotted against the momentum thickness in Fig. 8. Results from several forcing cases are included for comparison. The momentum thickness was scaled by the shortest forcing wavelength for the specific forcing condition, and the unforced case was scaled by the naturally most amplified wavelength. After the initial growth of the layer, the scaled total energy for all cases tends toward an asymptotic value of roughly 0.17, regardless of the mode of forcing. This indicates a limit on the specific total energy at equilibrium. At larger θ/λ, a slight oscillation of the specific total energy about the asymptote can be observed. Different modes of forcing can cause the energy to overshoot or undershoot initially. The forcing amplitude is also expected to be one of the controlling parameters of this initial response.

Summary and Conclusions

The behavior of a jet forced with combined frequencies at ratios of 1-2 and 1-3 has been studied using flow visualization and hot-wire measurements. For 1-2 forcing, if the initial growth of the longer wave is sufficiently strong compared with that of the shorter wave, three modes of vortex merging are possible: 1) pairing between two vortices of similar size, 2) pairing between two vortices of different size, and 3) vortex tearing. Both the initial phase angle and the Strouhal number play a key role in determining the mode of vortex emerging. Furthermore, modifications of the shear layer by different vortex merging modes result in different growth rates for the subharmonic of the longer wave, causing a rapid growth of the layer under certain forcing conditions. When forced at the condition where the first mode is close to the initially most amplified frequency, no vortex tearing can be observed, and vortex pairing occurs mostly between vortices of similar sizes. The phase angle affects mainly the pairing location in this situation. In general, for the cases studied, forcing at two growth modes at a ratio of 1-2 results in a faster growth of the layer than forcing by either frequency alone at the same overall forcing level.

For 1-3 forcing, three merging modes are identified. For the three initial vortices that will merge eventually, either the two leading vortices will pair first and then the resultant vortex pairs again with the trailing vortex, or the two trailing ones will pair first and then pair with the leading one, or all three will merge simultaneously. The simultaneous merging mode leads to the slowest layer growth after the first mode is saturated. The initial phase angle has a major effect in determining the merging mode. Forcing at two frequencies again leads to faster growth of the layer when compared with forc-

ing at one frequency alone. Regardless of the mode of forcing, the specific total energy tends toward the same asymptotic value of 0.17.

References

[1]Roshko, A., "Structure of Turbulent Shear Flow: A New Look," *AIAA Journal,* Vol. 14, Dec. 1976, pp. 1349–1357.

[2]Winant, C.D. and Browand, F.K., "Vortex Pairing, the Mechanism of Turbulent Mixing-Layer Growth at Moderate Reynolds Number," *Journal of Fluid Mechanics,* Vol. 63, Pt. 2, July 1974, pp. 237–255.

[3]Hernan, M.A. and Jimenez, J., "Computer Analysis of a High-Speed Film of the Plane Turbulent Mixing Layer," *Journal of Fluid Mechanics,* Vol. 119, June 1982, pp. 323–345.

[4]Miksad, R.W., "Experiments on the Nonlinear Stages of Free-Shear-Layer Transition," *Journal of Fluid Mechanics,* Vol. 56, Pt. 4, Feb. 1972, pp. 695–719.

[5]Miksad, R.W., "Experiments on Nonlinear Interactions in the Transition of a Free Shear Layer," *Journal of Fluid Mechanics,* Vol. 59, Pt. 1, July 1973, pp. 1–21.

[6]Zaman, K.B.M.Q. and Hussain, A.K.M.F., "Vortex Pairing in a Circular Jet Under Controlled Excitation. Part I. General Jet Response," *Journal of Fluid Mechanics,* Vol. 101, Pt. 3, Dec. 1980, pp. 449–491.

[7]Zaman, K.B.M.Q. and Hussain, A.K.M.F., "Turbulence Suppression in Free Shear Flows by Controlled Excitation," *Journal of Fluid Mechanics,* Vol. 103, July 1981, pp. 133–159.

[8]Ho, C.M. and Huang, L.S., "Subharmonics and Vortex Merging in Mixing Layers," *Journal of Fluid Mechanics,* Vol. 119, June 1982, pp. 443–473.

[9]Oster, D. and Wygnanski, I., "The Forced Mixing Layer Between Parallel Streams," *Journal of Fluid Mechanics,* Vol. 123, Oct. 1982, pp. 91–130.

[10]Ho, C.M. and Huerre, P., "Perturbed Free Shear Layers," *Annual Review of Fluid Mechanics,* Vol. 16, 1984, pp. 365–424.

[11]Wygnanski, I. and Petersen, R.A., "Coherent Motion in Excited Free Shear Flows," *AIAA Journal,* Vol. 25, Feb. 1987, pp. 201–213.

[12]Zhang, Y.Q., Ho, C.M., and Monkewitz, P., "The Mixing Layer Forced by Fundamental and Subharmonic," *Proceedings of IUTAM Symposium on Laminar-Turbulent Transition,* Springer-Verlag, Berlin, 1985, pp. 385–395.

[13]Patnaik, P.C., Sherman, F.S., and Corcos, G.M., "A Numerical Simulation of Kelvin-Helmholtz Waves of Finite Amplitude," *Journal of Fluid Mechanics,* Vol. 73, Pt. 2, July 1976, pp. 215–240.

[14]Riley, J.J. and Metcalfe, R.W., "Direct Numerical Simulation of a Perturbed Turbulent Mixing Layer," AIAA Paper 80-0274, Jan. 1980.

[15]Mankbadi, R.R., "The Effect of Phase-Difference on the Spread Rate of a Laminar Circular Jet Under Bi-modal Excitation," AIAA Paper 85-0045, Jan. 1985.

[16]Cain, A.B. and Thompson, M.W., "Linear and Weakly Nonlinear Aspects of Free Shear Layer Instability, Roll-up, Subharmonic Interaction and Wall Influence," AIAA Paper 86-1047, May 1986.

[17]Bradley, T.A., "The Effects of Forcing on the Near Field Development of a Circular Jet," M.S. Thesis, University of Notre Dame, Notre Dame, IN, 1987.

[18]Monkewitz, P.A. and Huerre, P., "The Influence of the Velocity Ratio on the Spatial Instability of Mixing Layers," *Physics of Fluids,* Vol. 25, July 1982, pp. 1137–1143.